HHS Public Access

Author manuscript

AJR Am J Roentgenol. Author manuscript; available in PMC 2016 May 16.

Published in final edited form as:

AJR Am J Roentgenol. 2012 January ; 198(1): 162–172. doi:10.2214/AJR.11.6505.

Proton MR Spectroscopy in Metabolic Assessment of Musculoskeletal Lesions

Ty K. Subhawong[1], **Xin Wang**, **Daniel J. Durand**, **Michael A. Jacobs**, **John A. Carrino**, **Antonio J. Machado**, and **Laura M. Fayad**

Russell H. Morgan Department of Radiology, and Radiological Science, Johns Hopkins Hospital, 601 N, Caroline St, Baltimore, MD 21287

Abstract

OBJECTIVE—The purposes of this review are to describe the principles and method of MR spectroscopy, summarize current published data on musculoskeletal lesions, and report additional cases that have been analyzed with recently developed quantitative methods.

CONCLUSION—Proton MR spectroscopy can be used to identify key tissue metabolites and may serve as a useful adjunct to radiographic evaluation of musculoskeletal lesions. A pooled analysis of 122 musculoskeletal tumors revealed that a discrete choline peak has a sensitivity of 88% and specificity of 68% in the detection of malignancy. Modest improvements in diagnostic accuracy in 22 of 122 cases when absolute choline quantification was used encourage the pursuit of development of choline quantification methods.

Keywords

choline; MRI; MR spectroscopy; musculoskeletal; tumor

Although MRI plays a central role in the assessment of musculoskeletal lesions, it lacks specificity for accurate differentiation of malignant from benign disease processes, particularly when fully determinate lesions such as lipomas and cysts are excluded [1–3]. MR spectroscopy (MRS) is a means of metabolic imaging with MRI that shows promise as a noninvasive method for molecular identification of malignant tumor markers. Such markers are potentially useful for a variety of applications, particularly characterization of musculoskeletal abnormalities to help guide treatment decisions [4–12]. Because benign lesions are encountered much more commonly than are malignant masses in a typical orthopedic clinic [13], an improved means of discriminating benign and malignant masses may obviate biopsy [14] and improve targeting of the most suspicious portion of a lesion being biopsied [4]. Although MRS is still primarily a research tool, improvements in spatial resolution, data acquisition, and data analysis techniques have allowed integration of MRS into clinical MRI examinations for preoperative lesion characterization and, potentially, posttreatment assessment [5, 6]. The purposes of this review are to elucidate the principles

[1]Address correspondence to T. K. Subhawong (tsubhaw1@jhmi.edu).

and method of MRS, summarize current published data on musculoskeletal lesions, and report additional cases in which analysis was performed with recently developed quantitative methods. The overall accuracy of MRS in the characterization of musculoskeletal lesions is described.

Proton (^{1}H) MR Spectroscopic Technique

Unlike the head, the almost uniform shape of which facilitates MRS of the brain, the body parts of the musculoskeletal system vary in size and shape, mandating flexibility in the use of coils. MRS is optimally performed with a surface coil because its sensitivity is three to five times that of a body coil. However, use of the body coil obviates use of an array of tailored surface coils, simplifies preimaging preparation, and increases anatomic coverage. Because of the inherently higher signal-to-noise ratio (SNR) at 3 T than at 1.5 T, further study is needed to determine whether a body coil can be used at 3 T to take advantage of these features without an unacceptable loss in SNR [5]. In either case, both the size of the region of interest and the tissue composition within it influence coil loading, making proper electrical calibration of coil efficiency an essential preimaging routine.

Shimming the local magnetic field is the most critical step in ensuring acquisition of high-quality spectra. For the musculoskeletal system, a manual shim is most effective because of the differences in extremity geometry and tissue heterogeneity compared with the brain. For example, musculoskeletal regions are composed of heterogeneous tissues with variable water and lipid content, magnetic homogeneity, susceptibility, and diffusion effects that affect resonance peak identification [15]. Although lipids are essentially absent from MR spectra in the brain, their abundance in the musculoskeletal system demands a longer TE, typically in the range of 130–150 ms (at 3 T), to avoid contamination of other metabolic peaks [7, 16]. The full width at half-maximum spectral line width is a good indicator of shimming. At our institution, this value varies considerably for different parts of the body (3-T MRI system, Verio, Siemens Healthcare). For example, 20–30 Hz of full width at half-maximum for thigh muscle, 30–40 Hz for trunk muscle, and 40–50 Hz for pelvic muscles indicate good shimming. A good symmetric water spectral profile after shimming should be used as a criterion in judging the adequacy of B_0 field homogeneity.

After appropriate shimming of the local magnetic field, the radiologist can choose either single-voxel or multivoxel spectroscopic imaging techniques for radiofrequency excitation in a volume of interest. Each approach has its advantages and disadvantages, which must be weighed in the context of the clinical situation. The benefits of the single-voxel technique are simplicity, shorter acquisition time, and easier maintenance of magnetic field homogeneity in the volume of interest. This volume can be defined by tuning the transmitter frequency and gradient pulse using sequences such as stimulated echo acquisition mode [17] and point-resolved spectroscopy [18]. In the multivoxel technique, phase-encoding gradients are applied in two or three directions, creating an array of voxel columns (2D chemical shift imaging) or volumes (3D chemical shift imaging). The multivoxel technique enables simultaneous acquisition of signals over a large FOV, providing information about the surrounding tissue, the possibility of analyzing multiple lesions at the same time, and improved sampling of heterogeneous tumors [19]. The last factor is particularly

advantageous in the management of tumors containing variable mixes of stroma, fat, and necrosis.

Volume selection is critical to proton (^{1}H) MRS of the musculoskeletal system because inclusion of too much subcutaneous fat can obscure the more subtle metabolic peaks of interest, and inclusion of vascular structures or cortical bone contaminates the ^{1}H spectra owing to signal dropout [20]. In our experience, skeletal tumors frequently replace the normal marrow, and although there is a danger of contamination from outer tissue voxels, good spectral quality is often obtained from skeletal lesions. In addition, contrast-enhanced sequences can be used to directly position the voxel of interest over well-vascularized and viable areas of tumor [21]. Findings by Lenkinski et al. [22] are evidence of exclusive use of neutral chelates of gadolinium in choline MRS to avoid underestimation of the choline peak if MRS is performed after contrast administration.

Proton MRS of musculoskeletal tumors in vivo has been performed at 1.5 T and 3 T but not at 7 T, to our knowledge. Theoretically, SNR and spectral resolution (chemical shift, measured in Hertz) increase linearly with B_0 magnetic field strength. However, decreases in T2 relaxation times and increased field inhomogeneity lead to increased metabolite line widths that significantly reduce the theoretically achievable gains in SNR at 3 T [23]. Losses in T2 relaxation time are exacerbated when a longer TE is used. A shorter TE, however, results in unacceptably large water and lipid peaks. Because of these considerations, an intermediate TE of 130–150 ms is an acceptable compromise between good sensitivity and shorter TE in the musculoskeletal system [5, 7]. The parameters of a representative protocol for MRS evaluation of a musculoskeletal tumor at our institution are summarized in Table 1.

Limitations

Although proton MRS is a promising technique that has been used successfully in the musculoskeletal system, a number of factors contribute to technical failure. Compared with the brain, musculoskeletal tissues are heterogeneous, causing greater variation in the local magnetic field inhomogeneity in the region of signal collection. Spectra from poorly shimmed examinations are marked by an increase in the coefficient of variation of measured metabolite concentrations [15]. To ensure consistency in spectral quality, shimming of the local magnetic field should optimally be performed for each patient. At our institution, active shimming is performed by an MR physicist and generally takes approximately 5–10 minutes for each examination.

In the musculoskeletal system, the use of different radiofrequency coils for different body parts results in a differential in gain in collected signal, which complicates the comparison of quantified results. Second, water, lipid, and tissue compartmentation is more heterogeneous in musculoskeletal tissues than in the brain. In the musculoskeletal system, not only water but also muscle and intramyocellular and extramyocellular lipids are the major compartments [20, 24–26]. Pathologic states can influence the water content of tissues in the voxel of interest and invalidate a priori assumptions about water concentration in quantitative models that entail a base set of metabolites (such as LCModel, Inverse Problems). Although some investigators have acquired spectra with water-suppressed

sequences only [8], we favor a strategy of water-suppressed and non–water-suppressed sequences to improve quantification of metabolite concentration.

Finally, the reproducibility of metabolite quantification has not been rigorously defined for musculoskeletal tissues. For metabolites in the brain, low-end estimates of coefficients of variation are in the range of 3–8%, allowing detection of differences in metabolite concentration as low as 12% in an individual over time [27], although higher estimates of coefficients of variation range from 8% to 20%, and are regionally dependent [28]. A preliminary study [7] showed coefficients of variation in the range of 5–17% for choline in the thigh, but additional work is needed to better define reproducibility for metabolite concentrations in musculoskeletal tissues.

Data Analysis

As in evaluation of the CNS, the main purpose of MRS in musculoskeletal applications is analysis of the metabolic profile of a lesion. Although qualitative [5, 19] and relative quantitative [4, 6, 9] techniques have been used to study certain metabolite changes, absolute quantification [8] in musculoskeletal tissues is needed. For quantification of any kind, data processing can be performed either in the time domain by direct processing of free induction decay signal or in the frequency domain after a Fourier transform. Although the approaches are mathematically equivalent, data are generally presented in the frequency domain to facilitate visual interpretation. Before quantification methods can be applied, preprocessing of the raw data generally is required. For example, low-pass filtering can reduce high-frequency background noise in the signal; apodizing in the time domain with digital filters can enhance features of the corresponding spectral model function (lorentzian, gaussian, or Voigt model) of the signal; and zero filling, or adding zeros at the end of the free induction delay signal, can improve the digital resolution and spectral appearance [29]. After a Fourier transform, convolution filtering can eliminate unwanted peaks due to noise in the spectra. Performance of spectral baseline correction reduces contamination from unwanted macromolecule signals. Time and frequency domain quantifications both fit the processed data into the corresponding mathematic model functions [30, 31]. Popular examples of quantitation software include Java Magnetic Resonance User Interface [32, 33], the Linear Combination of Model spectra (LCModel) [34], and MRI equipment vendor software, but discussion of the technical differences among these quantification algorithms is beyond the scope of this review.

Interpreting the results of quantification is closely correlated with the collection scheme. The area under the spectral resonance peak of a metabolite depends on the T1 and T2 relaxation properties of the metabolite. Thus, accurate quantification of the concentration of a metabolite necessitates correction of the particular influence of these relaxation properties on the strength of the resonance peak [7]. Initial quantification schemes involved comparing the area under the peak of a metabolite of unknown concentration to the area under the peak of a reference of known concentration after the T1 and T2 relaxation properties had been taken into account. Studies of musculoskeletal spectroscopy have included those with no concentration reference [8] and those incorporating an internal in vivo reference, such as water [7, 10].

Applications of MR Spectroscopy in the Musculoskeletal System

Although ^{31}P MRS has been used to characterize musculoskeletal tumors and their response to therapy [35], its spatial resolution and the need for special MRI hardware have limited its clinical utility. Proton (^{1}H) MRS does not have the problems of low abundance and low sensitivity that hinder the use of other nuclei, although it was initially hampered by large water and fat peaks that obscured the resonances of tissue metabolites [36]. Enhanced gradient performance and improved techniques of spectral analysis have allowed proton MRS to emerge as the method of choice for MRS of the musculoskeletal system because of its superior signal, superior spatial resolution, and technical simplicity for integrating MRS into clinical MRI examinations [20].

Proton MRS has been used to investigate numerous organ systems and disease processes. Although the intrinsic properties of the brain make this organ particularly amenable to MRS investigation of neoplastic, metabolic, and demyelinating diseases [37], MRS has also been used to probe the molecular characteristics in a variety of other tissues, such as breast [38], prostate [39], and liver [40]. With regard to the musculoskeletal system, proton MRS has been used to elucidate biochemical features of intramuscular lipid metabolism [41, 42] and intramuscular fat content in patients with rotator cuff tears [43] and chronic low back pain [44]. Only recently, however, has the utility of MRS in musculoskeletal tumor characterization been explored [4, 11, 12, 19, 45].

The underlying genetic aberrations acquired by neoplasms result in alterations of normal cellular biochemistry and metabolism [46]. Several methods have evolved for analysis of MRS results. These methods include qualitative (detection of metabolite peaks) and quantitative (measurement of metabolite ratios relative to noise or to other metabolites, measurement of metabolite concentration) approaches. An elevation in the rate of glycolysis, known as the Warburg effect, along with changes in lipid synthesis and oxidation, contribute to abnormal levels of lipids and other metabolites, such as choline and creatine, in tumors compared with normal tissue [47]. Spectroscopic analysis of lipid-to-water ratios in the bone marrow of leukemia patients has shown a higher relative water content than that in healthy subjects, reflective of an increase in the amount of hematopoietic tissue [48]. Oriol, et al. [49] examined 21 patients with multiple myeloma and found that only patients responding to treatment had a significant increase in bone marrow lipid-to-water ratio after therapy. However, it is the presence and quantitation of metabolites other than water or lipids that have served as the basis for spectroscopic analysis of brain tumors, in which more experience in MRS characterization has been gained than in analysis of the musculoskeletal system [37]. An early report by Oya et al. [45] showed that a peak in the region of *N*-acetyl aspartate increased in malignant tumors of neuroectodermal origin (such as clear cell sarcoma, Ewing sarcoma, and malignant schwannoma). More recent studies, however, have shown that the metabolite choline serves as a general marker of malignancy of musculoskeletal tumors [5, 9, 11]. Although proton MRS has shown intramuscular choline concentration altered in cases of myopathy and radiation injury [50], this review focuses on its role in characterization of musculoskeletal mass lesions.

Choline: A Metabolic Marker of Disease

Most MRS studies of musculoskeletal tumors have been focused on increased levels of choline in malignant bone and soft-tissue tumors [4–6, 9–12], an observation in agreement with evidence that choline is a useful marker of malignancy in several organ systems, including brain [37], breast [38], prostate [40], and liver [51]. For soft tissues, the biologic basis of these empiric observations has been found in in vitro studies showing that disorders that influence cell membrane turnover, such as uncontrolled proliferation in malignant transformation, result in changes in the concentration of choline-containing compounds [46]. These compounds are detectable with MRS as a discrete total choline peak at 3.2 ppm [52] (Fig. 1). This peak contains contributions from glycerophosphocholine, phosphocholine, and free choline, all of which are involved in the phospholipid metabolism of cell membranes (Fig. 2).

More specifically, gene microarray and in vitro MRS studies have shown that elevated choline concentration in tumors is primarily attributable to the accumulation of phosphocholine resulting from increases in choline kinase (choline → phosphocholine) and phospholipase (phosphatidylcholine → choline) expression and activity [53]. In addition to malignant transformation, hypoxia and pH changes in the tumor microenvironment can activate cell signaling pathways that result in increases in choline concentration detectable with MRS [54]. The choline peak at 3.2 ppm lies close to the creatine peak at 3.0 ppm. Both metabolites are abundant in normal muscle, requiring vigilance in ensuring appropriate voxel placement only within the tumor to avoid introducing contaminant signals from the surrounding tissue [5, 11].

Application 1: De Novo Tumor Characterization

Qualitative Assessment of Choline Content

In one of the first in vivo studies of proton MRS focusing on choline in musculoskeletal tumors, Wang et al. [11] examined with 1.5-T MRI 36 consecutively registered patients with tumors larger than 1.5 cm in diameter. In that study, choline was detected in 18 of 19 patients with malignant tumors and in 3 of 17 patients with benign lesions. These results yielded a sensitivity of 95%, specificity of 82%, and accuracy of 89% ($p < 0.001$).

Relative Quantification of Choline

Since the publication by Wang et al. [11], additional studies have shown false-positive choline peaks in benign giant cell tumors of bone [12] and a variety of other inflammatory or benign neoplastic processes [5, 6, 8, 9, 11, 12]. Because a subset of benign lesions is known to contain choline, there has been a focus on improving quantitative assessment of the choline level within musculoskeletal lesions with the aim of enhancing specificity [10]. Relative quantification methods include measurement of peak ratios between metabolites and between a metabolite and the background noise level (SNR). Initial strategies entailing SNR showed that good discrimination between malignant and benign lesions can be achieved. In a study of 13 ex vivo skeletal sarcoma specimens imaged at 1.5 T, Fayad et al. [4] found that the choline SNR was significantly different for histologically proven areas of

malignancy compared with nonmalignant tissue (9.8 ± 5.1 vs 2.7 ± 1.4, $p < 0.002$). These results suggest that MRS can be used to direct a biopsy to the most suspicious regions of a tumor. The preliminary data from this study revealed that choline content may correlate with histologic grade. Subsequently, an in vivo study [5] involving 18 patients (four with histologically proven malignant tumors, 14 with benign tumors histologically proven or confirmed at clinical follow-up) who underwent 3-T MRI with both single-voxel and multivoxel techniques also showed that the SNRs of malignant and benign lesions differed from each other (11.7 vs 2.3, $p = 0.04$). An example of a patient who underwent single-voxel MRS and relative choline quantitation with choline SNR is shown in Figure 3.

Despite the apparent success in use of the choline SNR for characterization of musculoskeletal lesions, a number of limitations are associated with use of SNR measurements. Choline signal intensity can vary with numerous factors, including pulse sequence, magnetic field strength, differences in coil type, distance between the region of interest and the coil, and the size of the lesion being analyzed. Although a relative comparison of peak ratios of different metabolites requires less acquisition time and less postprocessing than absolute quantitative methods, such a ratio does not indicate which metabolite concentration is abnormal. Moreover, systemic conditions in which there are global changes in metabolite concentrations can yield proportions that appear normal. In addition to this ambiguity, metabolite ratios can exhibit higher variation than absolute quantification [55, 56]. Finally, spectroscopic results expressed only as metabolite ratios may be of limited utility in comparisons with results of studies in which absolute concentrations are derived biochemically [57].

Absolute Quantification of Choline

The limitations of relative quantitation have prompted a search for alternative and more robust quantitative methods for measuring metabolite content in vivo, namely determination of metabolite concentration. Again, most experience with MRS quantitation techniques has been gained in study of the brain [37, 57]. These techniques generally involve comparison of in vivo metabolite signals from a region of interest with an external or internal reference of known concentration. For the external reference, a voxel is placed in a phantom solution containing a known concentration of a given metabolite, which must be situated near the in vivo region of interest [56]. In clinical use, however, this technique is suboptimal because it is time-consuming, labor intensive, and subject to variations in coil geometry and field inhomogeneity that adversely affect measurements. Alternatively, the use of an internal reference compound, such as water or fat, allows determination of chemical concentrations by comparison with a known endogenous compound with a defined concentration [7].

Reports on imaging of the musculoskeletal system describe absolute quantification of choline performed at 2 T and 3 T [58] and of creatine and lipids at 1.5 T [16, 59, 60]. With modification of previously described methods of choline quantification for evaluation of lesions in the brain and breast [61, 62], a robust method of measuring absolute choline concentration within the musculoskeletal system can be achieved with water as an internal reference compound [7]. In this water-referencing technique, both water-suppressed and non–water-suppressed images are acquired with a phased-array coil (Fig. 4). From these

data, the area under the choline and water peaks is used to generate the choline concentration, after correction for the variability of lipid content. By using this approach in a small sample of patients, Fayad et al. [10] found good discrimination between benign and malignant lesions (0.5 vs 2.7 mmol/ kg, $p = 0.01$) (Figs. 5–7).

A key assumption underlying this quantification method is that the water content is constant between voxels, lesions, and patients. Unfortunately, total water content in various musculoskeletal pathologic conditions is unlikely to be constant and even in normal muscle has been found to change slightly after exercise [63, 64]. Consequently, alternative quantitative techniques that surmount such limitations are needed.

Systematic Review of MR Spectroscopic Studies for Tumor Characterization

We searched the peer-reviewed literature via PubMed for articles in English published since January 2004 that described the use of ^{1}H MRS of the musculoskeletal system. The search terms and keywords used in our computerized search strategy were: MR spectroscopy, musculoskeletal, and tumor. Seven relevant articles were identified, but a study by Qi et al. [9] provided insufficient detail about individual cases for inclusion in numeric analysis (Table 2). The other studies comprised 122 musculoskeletal tumors or masslike lesions, some of which had been subjected to neoadjuvant therapy before spectroscopy. The results of the studies in which semiquantitative findings (SNR) or absolute metabolite concentrations were reported were dichotomized to facilitate overall comparison with qualitative data (reported as presence or absence of a choline peak). Although Lee et al. [8] did use absolute metabolite concentrations, only qualitative characterization could be extracted for each histologic diagnosis. We believe that because of variations in coil loading, shimming, and other collection conditions, absolute metabolite concentrations from that study cannot be rigorously compared with results in other publications.

A pooled analysis of MRS studies of de novo musculoskeletal lesions (Table 3) shows a strong association between the presence of a choline peak and malignancy ($p < 0.0001$, Fisher exact test) with a sensitivity of 88% and a specificity of 68%. The corresponding positive (PPV) and negative (NPV) predictive values for malignancy in the presence of a discrete choline peak are 73% and 86%. In particular, a summary of the cases to date shows that two tumors (giant cell tumor and peripheral nerve sheath tumor) accounted for 15 of 20 benign lesions with discrete choline peaks. Caution should be exercised in the interpretation of such entities to avoid overcalling malignancy on the basis of qualitative MRS data alone [5, 8, 11, 12].

Improved quantitative methods have been pursued with the aim of increasing the specificity of MRS. A subanalysis of results of the 25 published cases in which choline SNR was provided [4, 5] showed 81% sensitivity and 78% specificity when a theoretic cutoff of 5 was used to suggest malignancy; the PPV was 87% and the NPV 70% (Table 4). The area under the curve for receiver operating characteristic analysis of SNR as a marker for malignancy was 0.93 (Fig. 8A). (As discussed earlier, however, using choline SNR as a quantitative tool is limited because of the variety of factors that influence SNR.) With absolute choline concentration as a quantitative discriminator of benign and malignant disease, we analyzed 15 published [10] and seven unpublished cases from our institution. A threshold choline

concentration of 0.3 mmol/kg to define malignancy resulted in a sensitivity of 100%, specificity of 81%, PPV of 73%, and NPV of 100%. A threshold choline concentration of 0.8 mmol/ kg to define malignancy resulted in a sensitivity of 88%, specificity of 88%, PPV of 78%, and NPV of 93% (Table 4). For this small series of cases, the area under the ROC curve for absolute choline concentration remained high at 0.95 (Fig. 8B).

With regard to characterizing tumor grade, although Fayad et al. [4] found correlation between choline SNR measurements and tumor grade [4], Lee et al. [8] found that absolute choline concentration does not correlate well with the histologic grade of malignant lesions, although the small number and heterogeneity of tumor types in this analysis warrant further study.

Although technologic advances may lead to improvement in the accuracy of MRS in discriminating benign and malignant lesions, the observed reasonable specificity and high NPV of extant data already are promising evidence that lack of detection of an elevated choline concentration in a lesion may allow a carefully selected subset of patients to forgo biopsy in favor of close observation when a benign cause is suspected. Quantitative MRS may prove especially useful in specific populations of patients with tumors that occasionally present diagnostic dilemmas.

Application 2: Treatment Response

Limited preliminary experience has been gained in using choline concentration to monitor treatment response in musculoskeletal disease. Hsieh et al. [6] reported that declining choline concentration correlated with a decrease in tumor size and dynamic contrast enhancement after chemotherapy in two patients with aggressive musculoskeletal tumors. Because percentage of tumor necrosis is known to be the strongest predictor of treatment response for soft-tissue sarcoma and primary malignant tumors of bone [65, 66], these observations raise the possibility that through early detection of changes in choline content, MRS may play a role in assessing prognosis through quantification of the degree of tumor necrosis. To this end, our group’s preliminary data include detection of choline (0.6 mmol/kg) in one poorly responsive osteosarcoma (only 10% histologic necrosis) and lack of a discrete choline peak in three chemotherapy-responsive malignant tumors (two Ewing sarcomas and one malignant fibrous histiocytoma, each with 100% histologic necrosis). However, the pretreatment choline concentration of these lesions was not ascertained.

Application 3: Postsurgical Evaluation

Conventional MRI plays a pivotal role in the postoperative assessment of resected tumors for determination of the presence of residual or recurrent disease [67]. It can be challenging, however, to identify recurrent tumor in the postoperative milieu of changes in the surgical bed. Only when the patient has a mature postsurgical scar can one confidently exclude recurrent disease by noting the absence of T2 signal intensity [68]. Unfortunately, reconstructive myocutaneous flaps have T2 hyperintensity for 6–12 months or more, increasing the complexity of detection of recurrent and residual tumor in the resection bed. To address these difficulties, research has been conducted on the utility of postoperative

proton MRS. Fayad, et al. [5] found that in six postoperative patients without evidence of recurrent or residual tumor at clinical follow-up and conventional MRI, proton MRS showed two spectral patterns. When myocutaneous flap reconstruction had been performed, MRS of the surgical bed revealed the typical spectrum of muscle. In surgical cases in which myocutaneous flap reconstruction had not been performed, only lipid and water signals were found in patients without recurrent disease, and a discrete choline signal was lacking. Subsequent study of absolute quantitative methods to assess choline postoperative concentration [12] has shown negligible to very low amounts of choline (up to 0.4 mmol/kg) in disease-free patients, but no myocutaneous flap reconstructions were included in that study.

Conclusion

The increased clinical use of high-field-strength magnets coupled with improvements in pulse sequence design and quantitative methods promises to move MRS from the realm of research to clinical practice in the field of musculoskeletal imaging. The versatility of the technique allows a range of metabolites to be assessed in a variety of disorders, although this review has focused on neoplastic conditions. Absolute quantification of choline concentration shows early promise as an adjunct to conventional imaging in differentiating benign from malignant musculoskeletal abnormalities in de novo lesions and may play a role in prediction of therapeutic response in the postoperative setting. Further studies are needed to elucidate how the variability in relative water content and choline concentration in different disease states and among individuals influences determination of metabolite concentration and how these factors affect the utility of MRS in discriminating malignant changes both before and after treatment.

Acknowledgments

T. K. Subhawong supported by NIH grant 1T32EB006351. Other awards include the William M. G. Gatewood, M.D., Fellowship and the SCBT/MR Young Investigator’s Award. M. A. Jacobs supported by NIH grants R01CA100184, P50CA103175, 5P30CA06973, Breast SPORE CA88843, Avon:01-2009-031, and U01CA070095. L. Fayad supported by the GE Healthcare Radiology Research Fellowship.

References

1. Berquist TH, Ehman RL, King BF, Hodgman CG, Ilstrup DM. Value of MR imaging in differentiating benign from malignant soft-tissue masses: study of 95 lesions. AJR. 1990; 155:1251–1255. [PubMed: 2122675]
2. Crim JR, Seeger LL, Yao L, Chandnani V, Eckardt JJ. Diagnosis of soft-tissue masses with MR imaging: can benign masses be differentiated from malignant ones? Radiology. 1992; 185:581–586. [PubMed: 1410377]
3. Gielen JL, De Schepper AM, Vanhoenacker F, et al. Accuracy of MRI in characterization of soft tissue tumors and tumor-like lesions: a prospective study in 548 patients. Eur Radiol. 2004; 14:2320–2330. [PubMed: 15290067]
4. Fayad LM, Bluemke DA, McCarthy EF, Weber KL, Barker PB, Jacobs MA. Musculoskeletal tumors: use of proton MR spectroscopic imaging for characterization. J Magn Reson Imaging. 2006; 23:23–28. [PubMed: 16315208]
5. Fayad LM, Barker PB, Jacobs MA, et al. Characterization of musculoskeletal lesions on 3-T proton MR spectroscopy. AJR. 2007; 188:1513–1520. [PubMed: 17515370]

6. Hsieh TJ, Li CW, Chuang HY, Liu GC, Wang CK. Longitudinally monitoring chemotherapy effect of malignant musculoskeletal tumors with in vivo proton magnetic resonance spectroscopy: an initial experience. J Comput Assist Tomogr. 2008; 32:987–994. [PubMed: 19204465]
7. Fayad LM, Salibi N, Wang X, et al. Quantification of muscle choline concentrations by proton MR spectroscopy at 3 T: technical feasibility. AJR. 2010; 194:228. [web]W73–W79.
8. Lee CW, Lee J, Kim DH, et al. Proton magnetic resonance spectroscopy of musculoskeletal lesions at 3 T with metabolite quantification. Clin Imaging. 2010; 34:47–52. [PubMed: 20122519]
9. Qi ZH, Li CF, Li ZF, Zhang K, Wang Q, Yu DX. Preliminary study of 3T ^{1}H MR spectroscopy in bone and soft tissue tumors. Chin Med J (Engl). 2009; 122:39–43. [PubMed: 19187615]
10. Fayad LM, Wang X, Salibi N, et al. A feasibility study of quantitative molecular characterization of musculoskeletal lesions by proton MR spectroscopy at 3 T. AJR. 2010; 195:207. [web]W69-W75.
11. Wang CK, Li CW, Hsieh TJ, Chien SH, Liu GC, Tsai KB. Characterization of bone and soft-tissue tumors with in vivo ^{1}H MR spectroscopy: initial results. Radiology. 2004; 232:599–605. [PubMed: 15286325]
12. Sah PL, Sharma R, Kandpal H, et al. In vivo proton spectroscopy of giant cell tumor of the bone. AJR. 2008; 190:433. [web]W133-W139.
13. Damron TA, Beauchamp CP, Rougraff BT, Ward WG Sr. Soft-tissue lumps and bumps. Instr Course Lect. 2004; 53:625–637. [PubMed: 15116652]
14. Mankin HJ, Mankin CJ, Simon MA. The hazards of the biopsy, revisited. Members of the Musculoskeletal Tumor Society. J Bone Joint Surg Am. 1996; 78:656–663. [PubMed: 8642021]
15. De Graaf, RA. In vivo NMR spectroscopy: principles and techniques. 2nd ed.. West Sussex, England: Wiley; 2007.
16. Bottomley PA, Lee Y, Weiss RG. Total creatine in muscle: imaging and quantification with proton MR spectroscopy. Radiology. 1997; 204:403–410. [PubMed: 9240527]
17. Frahm J, Bruhn H, Gyngell ML, Merboldt KD, Hänicke W, Sauter R. Localized high-resolution proton NMR spectroscopy using stimulated echoes: initial applications to human brain in vivo. Magn Reson Med. 1989; 9:79–93. [PubMed: 2540396]
18. Bottomley PA. Spatial localization in NMR spectroscopy in vivo. Ann N Y Acad Sci. 1987; 508:333–348. [PubMed: 3326459]
19. Fayad LM, Barker PB, Bluemke DA. Molecular characterization of musculoskeletal tumors by proton MR spectroscopy. Semin Musculoskelet Radiol. 2007; 11:240–245. [PubMed: 18260034]
20. Boesch C. Musculoskeletal spectroscopy. J Magn Reson Imaging. 2007; 25:321–338. [PubMed: 17260389]
21. Wang CK, Hsieh TJ, Jaw TS, Lin JN, Liu GC, Li CW. Clinical application of in vivo proton (1 H) MR spectroscopy in musculoskeletal tumors. Spectroscopy. 2005; 19:181–190.
22. Lenkinski RE, Wang X, Elian M, Goldberg SN. Interaction of gadolinium-based MR contrast agents with choline: implications for MR spectroscopy (MRS) of the breast. Magn Reson Med. 2009; 61:1286–1292. [PubMed: 19365855]
23. Barker PB, Hearshen DO, Boska MD. Single-voxel proton MRS of the human brain at 1.5 T and 3.0 T. Magn Reson Med. 2001; 45:765–769. [PubMed: 11323802]
24. Machann J, Stefan N, Schick F. (1)H MR spectroscopy of skeletal muscle, liver and bone marrow. Eur J Radiol. 2008; 67:275–284. [PubMed: 18406092]
25. Boesch C, Machann J, Vermathen P, Schick F. Role of proton MR for the study of muscle lipid metabolism. NMR Biomed. 2006; 19:968–988. [PubMed: 17075965]
26. Natt O, Bezkorovaynyy V, Michaelis T, Frahm J. Use of phased array coils for a determination of absolute metabolite concentrations. Magn Reson Med. 2005; 53:3–8. [PubMed: 15690495]
27. Brooks WM, Friedman SD, Stidley CA. Reproducibility of ^{1}H-MRS in vivo. Magn Reson Med. 1999; 41:193–197. [PubMed: 10025629]
28. Jansen JF, Kooi ME, Kessels AG, Nicolay K, Backes WH. Reproducibility of quantitative cerebral T2 relaxometry, diffusion tensor imaging, and ^{1}H magnetic resonance spectroscopy at 3.0 Tesla. Invest Radiol. 2007; 42:327–337. [PubMed: 17507802]
29. in 't Zandt H, van Der Graaf M, Heerschap A. Common processing of in vivo MR spectra. NMR Biomed. 2001; 14:224–232. [PubMed: 11410940]

30. Mierisová S, Ala-Korpela M. MR spectroscopy quantitation: a review of frequency domain methods. NMR Biomed. 2001; 14:247–259. [PubMed: 11410942]
31. Vanhamme L, Sundin T, Hecke PV, Huffel SV. MR spectroscopy quantitation: a review of time-domain methods. NMR Biomed. 2001; 14:233–246. [PubMed: 11410941]
32. Naressi A, Couturier C, Castang I, de Beer R, Graveron-Demilly D. Java-based graphical user interface for MRUI, a software package for quantitation of in vivo/medical magnetic resonance spectroscopy signals. Comput Biol Med. 2001; 31:269–286. [PubMed: 11334636]
33. Naressi A, Couturier C, Devos JM, et al. Java-based graphical user interface for the MRUI quantitation package. MAGMA. 2001; 12:141–152. [PubMed: 11390270]
34. Provencher SW. Estimation of metabolite concentrations from localized in vivo proton NMR spectra. Magn Reson Med. 1993; 30:672–679. [PubMed: 8139448]
35. Sostman HD, Prescott DM, Dewhirst MW, et al. MR imaging and spectroscopy for prognostic evaluation in soft-tissue sarcomas. Radiology. 1994; 190:269–275. [PubMed: 8259418]
36. Kreis R, Boesch C. Spatially localized, one- and two-dimensional NMR spectroscopy and in vivo application to human muscle. J Magn Reson B. 1996; 113:103–118. [PubMed: 8948135]
37. Zhu H, Barker PB. MR spectroscopy and spectroscopic imaging of the brain. Methods Mol Biol. 2011; 711:203–226. [PubMed: 21279603]
38. Jacobs MA, Barker PB, Bottomley PA, Bhujwalla Z, Bluemke DA. Proton magnetic resonance spectroscopic imaging of human breast cancer: a preliminary study. J Magn Reson Imaging. 2004; 19:68–75. [PubMed: 14696222]
39. Klijn S, De Visschere PJ, De Meerleer GO, Villeirs GM. Comparison of qualitative and quantitative approach to prostate MR spectroscopy in peripheral zone cancer detection. Eur J Radiol. 2011 Jan 5. [Epub ahead of print].
40. Fischbach F, Bruhn H. Assessment of in vivo ^{1}H magnetic resonance spectroscopy in the liver: a review. Liver Int. 2008; 28:297–307. [PubMed: 18290772]
41. Bredella MA, Ghomi RH, Thomas BJ, Miller KK, Torriani M. Comparison of 3.0 T proton magnetic resonance spectroscopy short and long echo-time measures of intramyocellular lipids in obese and normal-weight women. J Magn Reson Imaging. 2010; 32:388–393. [PubMed: 20677267]
42. Torriani M, Thomas BJ, Halpern EF, Jensen ME, Rosenthal DI, Palmer WE. Intramyocellular lipid quantification: repeatability with ^{1}H MR spectroscopy. Radiology. 2005; 236:609–614. [PubMed: 16040916]
43. Pfrrmann CWA, Schmid MR, Zanetti M, Jost B, Gerber C, Hodler J. Assessment of fat content in supraspinatus muscle with proton MR spectroscopy in asymptomatic volunteers and patients with supraspinatus tendon lesions. Radiology. 2004; 232:709–715. [PubMed: 15333791]
44. Mengiardi B, Schmid MR, Boos N, et al. Fat content of lumbar paraspinal muscles in patients with chronic low back pain and in asymptomatic volunteers: quantification with MR spectroscopy. Radiology. 2006; 240:786–792. [PubMed: 16926328]
45. Oya N, Aoki J, Shinozaki T, Watanabe H, Takagishi K, Endo K. Preliminary study of proton magnetic resonance spectroscopy in bone and soft tissue tumors: an unassigned signal at 2.0–2.1 ppm may be a possible indicator of malignant neuroectodermal tumor. Radiat Med. 2000; 18:193–198. [PubMed: 10972550]
46. Aboagye EO, Bhujwalla ZM. Malignant transformation alters membrane choline phospholipid metabolism of human mammary epithelial cells. Cancer Res. 1999; 59:80–84. [PubMed: 9892190]
47. Canese R, Iorio E, Ricci A, Pisanu ME, Giannini M, Podo F. Metabolite quantification in tumours by magnetic resonance spectroscopy: objectives, results and perspectives. Curr Med Imaging Rev. 2009; 5:110–127.
48. Jensen KE, Jensen M, Grundtvig P, Thomsen C, Karle H, Henriksen O. Localized in vivo proton spectroscopy of the bone marrow in patients with leukemia. Magn Reson Imaging. 1990; 8:779–789. [PubMed: 2266805]
49. Oriol A, Valverde D, Capellades J, Cabañas ME, Ribera J, Arús C. In vivo quantification of response to treatment in patients with multiple myeloma by ^{1}H magnetic resonance spectroscopy of bone marrow. MAGMA. 2007; 20:93–101. [PubMed: 17410391]

50. Bongers H, Schick F, Skalej M, Jung WI, Stevens A. Localized in vivo ^{1}H spectroscopy of human skeletal muscle: normal and pathologic findings. Magn Reson Imaging. 1992; 10:957–964. [PubMed: 1461093]
51. Li CW, Kuo YC, Chen CY, et al. Quantification of choline compounds in human hepatic tumors by proton MR spectroscopy at 3 T. Magn Reson Med. 2005; 53:770–776. [PubMed: 15799049]
52. Herminghaus S, Pilatus U, Möller-Hartmann W, et al. Increased choline levels coincide with enhanced proliferative activity of human neuroepithelial brain tumors. NMR Biomed. 2002; 15:385–392. [PubMed: 12357552]
53. Glunde K, Jie C, Bhujwalla ZM. Molecular causes of the aberrant choline phospholipid metabolism in breast cancer. Cancer Res. 2004; 64:4270–4276. [PubMed: 15205341]
54. Glunde K, Shah T, Winnard PT, et al. Hypoxia regulates choline kinase expression through hypoxia-inducible factor-1 alpha signaling in a human prostate cancer model. Cancer Res. 2008; 68:172–180. [PubMed: 18172309]
55. Li BS, Wang H, Gonen O. Metabolite ratios to assumed stable creatine level may confound the quantification of proton brain MR spectroscopy. Magn Reson Imaging. 2003; 21:923–928. [PubMed: 14599543]
56. Minati L, Aquino D, Bruzzone MG, Erbetta A. Quantitation of normal metabolite concentrations in six brain regions by in-vivo H-MR spectroscop y. J Med Phys. 2010; 35:154–163. [PubMed: 20927223]
57. Jansen JF, Backes WH, Nicolay K, Kooi ME. ^{1}H MR spectroscopy of the brain: absolute quantification of metabolites. Radiology. 2006; 240:318–332. [PubMed: 16864664]
58. Bruhn H, Frahm J, Gyngell ML, Merboldt KD, Hänicke W, Sauter R. Localized proton NMR spectroscopy using stimulated echoes: applications to human skeletal muscle in vivo. Magn Reson Med. 1991; 17:82–94. [PubMed: 1648655]
59. Rico-Sanz J, Hajnal JV, Thomas EL, Mierisová S, Ala-Korpela M, Bell JD. Intracellular and extracellular skeletal muscle triglyceride metabolism during alternating intensity exercise in humans. J Physiol. 1998; 510:615–622. [PubMed: 9706008]
60. Bárány M, Venkatasubramanian PN, Mok E, et al. Quantitative and qualitative fat analysis in human leg muscle of neuromuscular diseases by ^{1}H MR spectroscopy in vivo. Magn Reson Med. 1989; 10:210–226. [PubMed: 2761380]
61. Baik HM, Su MY, Yu H, Mehta R, Nalcioglu O. Quantification of choline-containing compounds in malignant breast tumors by ^{1}H MR spectroscopy using water as an internal reference at 1.5 T. MAGMA. 2006; 19:96–104. [PubMed: 16779565]
62. Soher BJ, Hurd RE, Sailasuta N, Barker PB. Quantitation of automated single-voxel proton MRS using cerebral water as an internal reference. Magn Reson Med. 1996; 36:335–339. [PubMed: 8875401]
63. Fotedar LK, Slopis JM, Narayana PA, Fenstermacher MJ, Pivarnik J, Butler IJ. Proton magnetic resonance of exercise-induced water changes in gastrocnemius muscle. J Appl Physiol. 1990; 69:1695–1701. [PubMed: 2177054]
64. Forsberg AM, Nilsson E, Werneman J, Bergström J, Hultman E. Muscle composition in relation to age and sex. Clin Sci (Lond). 1991; 81:249–256. [PubMed: 1716189]
65. Eilber FC, Rosen G, Eckardt J, et al. Treatment-induced pathologic necrosis: a predictor of local recurrence and survival in patients receiving neoadjuvant therapy for high-grade extremity soft tissue sarcomas. J Clin Oncol. 2001; 19:3203–3209. [PubMed: 11432887]
66. Davis AM, Bell RS, Goodwin PJ. Prognostic factors in osteosarcoma: a critical review. J Clin Oncol. 1994; 12:423–431. [PubMed: 8113851]
67. De Schepper AM, De Beuckeleer L, Vandevenne J, Somville J. Magnetic resonance imaging of soft tissue tumors. Eur Radiol. 2000; 10:213–223. [PubMed: 10663750]
68. Vanel D, Lacombe MJ, Couanet D, Kalifa C, Spielmann M, Genin J. Musculoskeletal tumors: follow-up with MR imaging after treatment with surgery and radiation therapy. Radiology. 1987; 164:243–245. [PubMed: 3588913]

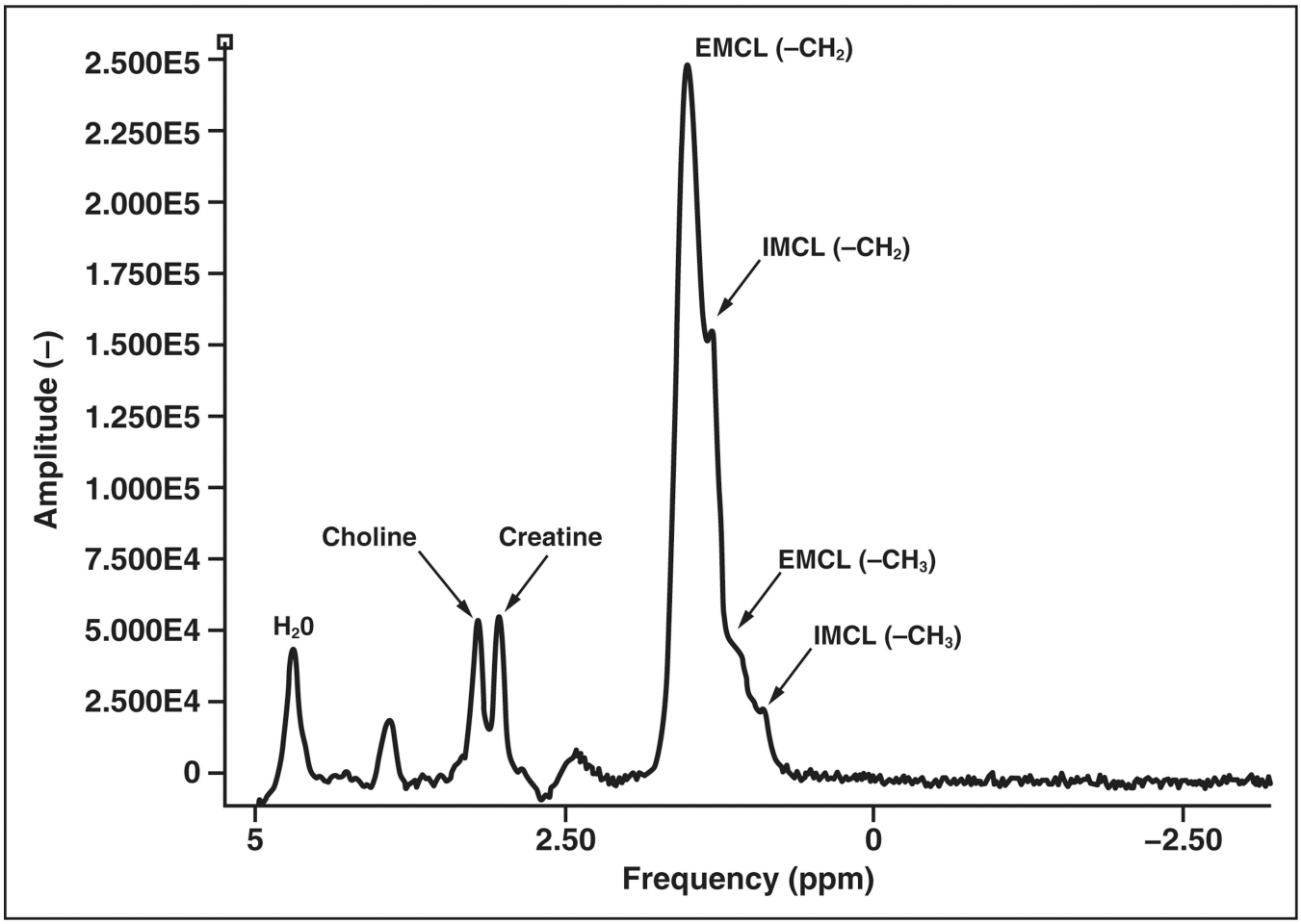

Figure 1.

Graph shows protons in different molecules resonate at different frequencies, which are mapped to specific location in parts per million (ppm). Typical ^{1}H MR spectrum of normal muscle shows following metabolites: water (H_2O), choline creatine, and intramyocellular (IMCL) and extramyocellular (EMCL) lipids. Choline (metabolite marker for malignancy) has peak at approximately 3.2 ppm. Relative measure of choline signal intensity with respect to noise (between 7 and 9 ppm, not shown) has been used to quantify choline content but has limitations.

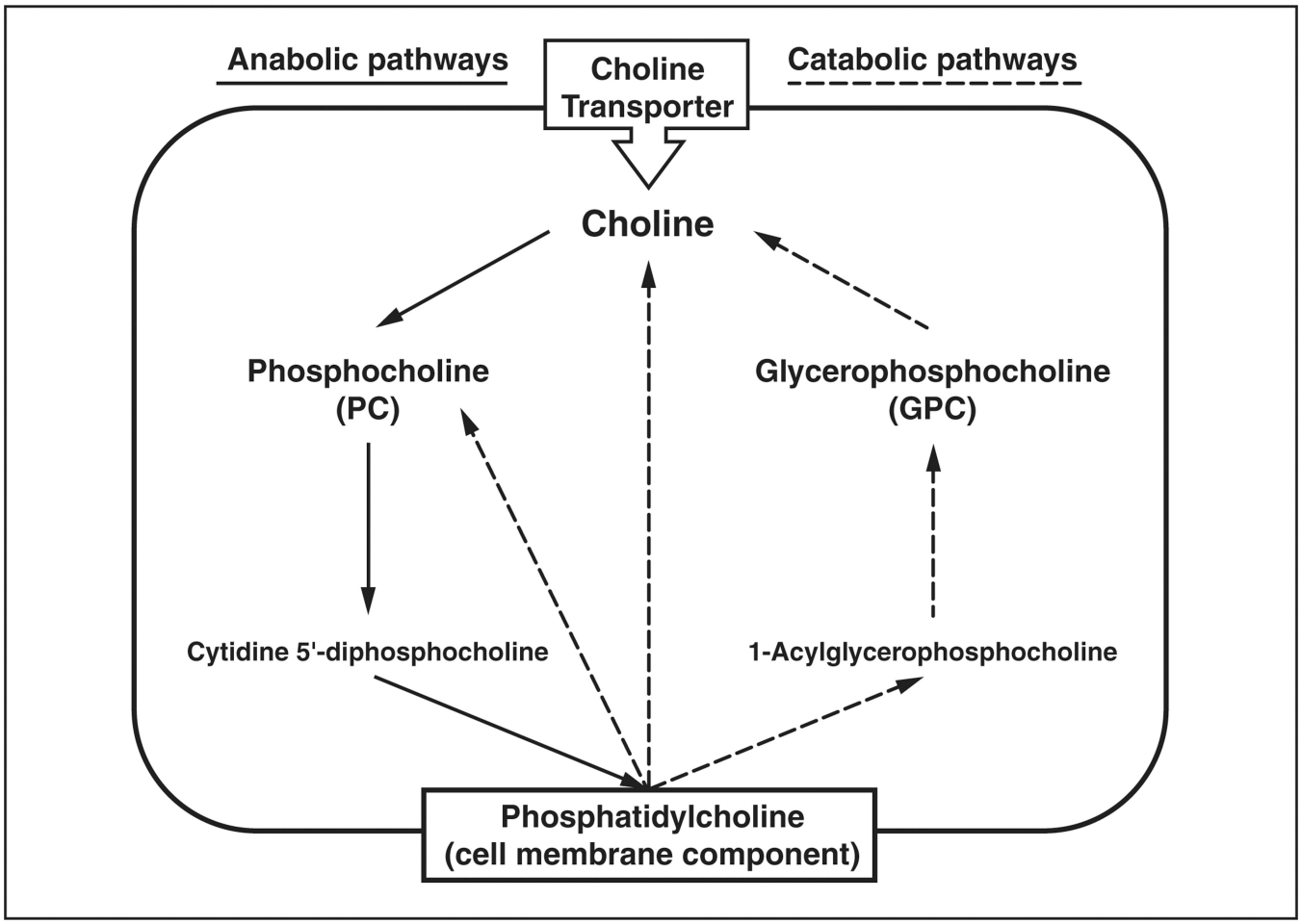

Figure 2.

Diagram shows major pathways in cellular choline metabolism listing only major metabolites (enzymes, precursors, cofactors, and byproducts omitted). Bold type indicates metabolites that contribute to total choline peak during proton MR spectroscopy. Elevated choline concentration in tumors is believed to be primarily due to accumulation of phosphocholine resulting from increases in activity of choline kinase (choline → phosphocholine) and phospholipase (phosphatidylcholine → choline).

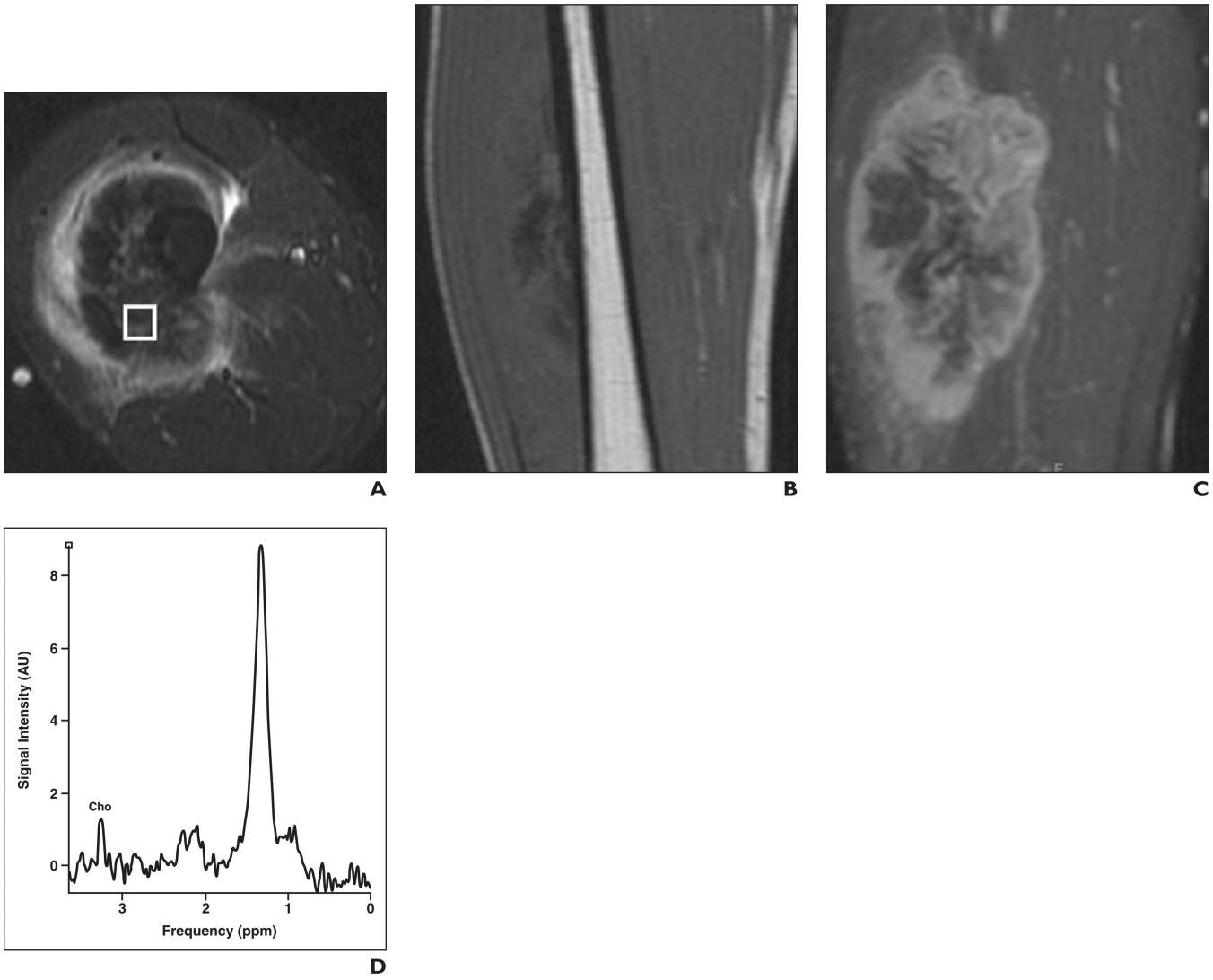

Figure 3.

31-year-old man with high-grade osteosarcoma of right thigh.

A, Axial STIR fast spin-echo MR image (TR/TE, 4650/47) shows large heterogeneous mass in anterolateral right thigh with surrounding soft-tissue edema.

B, Coronal T1-weighted spin-echo MR image (TR/TE, 550/11) shows low-signal-intensity mass.

C, Coronal fat-saturated dynamic contrast-enhanced fast spin-echo MR image (TR/TE, 600/10) acquired 40 seconds after contrast injection shows heterogeneous enhancement with central areas of necrosis.

D, Single-voxel MR spectroscopic map shows discrete choline (Cho) peak at 3.2 ppm. Signal-to-noise ratio is 5.4.

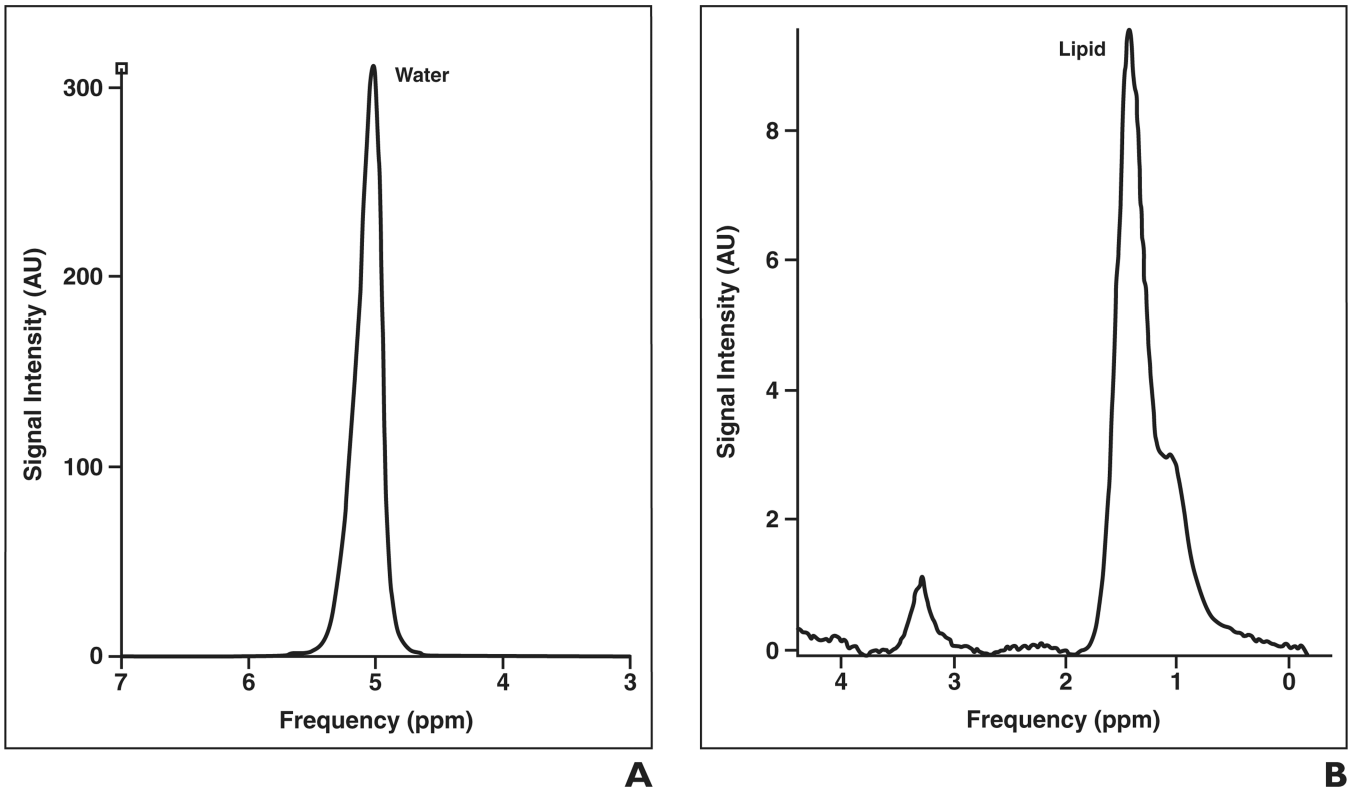

Figure 4.

Water referencing technique for absolute quantification of choline (Cho).

A and **B**, Graphs of non–water-suppressed (**A**) and water-suppressed (**B**) MR acquisitions show water suppression allows discrimination of choline signal intensity. From these data, areas under choline and water peaks are determined and used to calculate choline concentration based on T1 and T2 relaxation times of choline and water, number of protons attached to choline and water, and correction factors for lipid in voxel and water content of tissue [7].

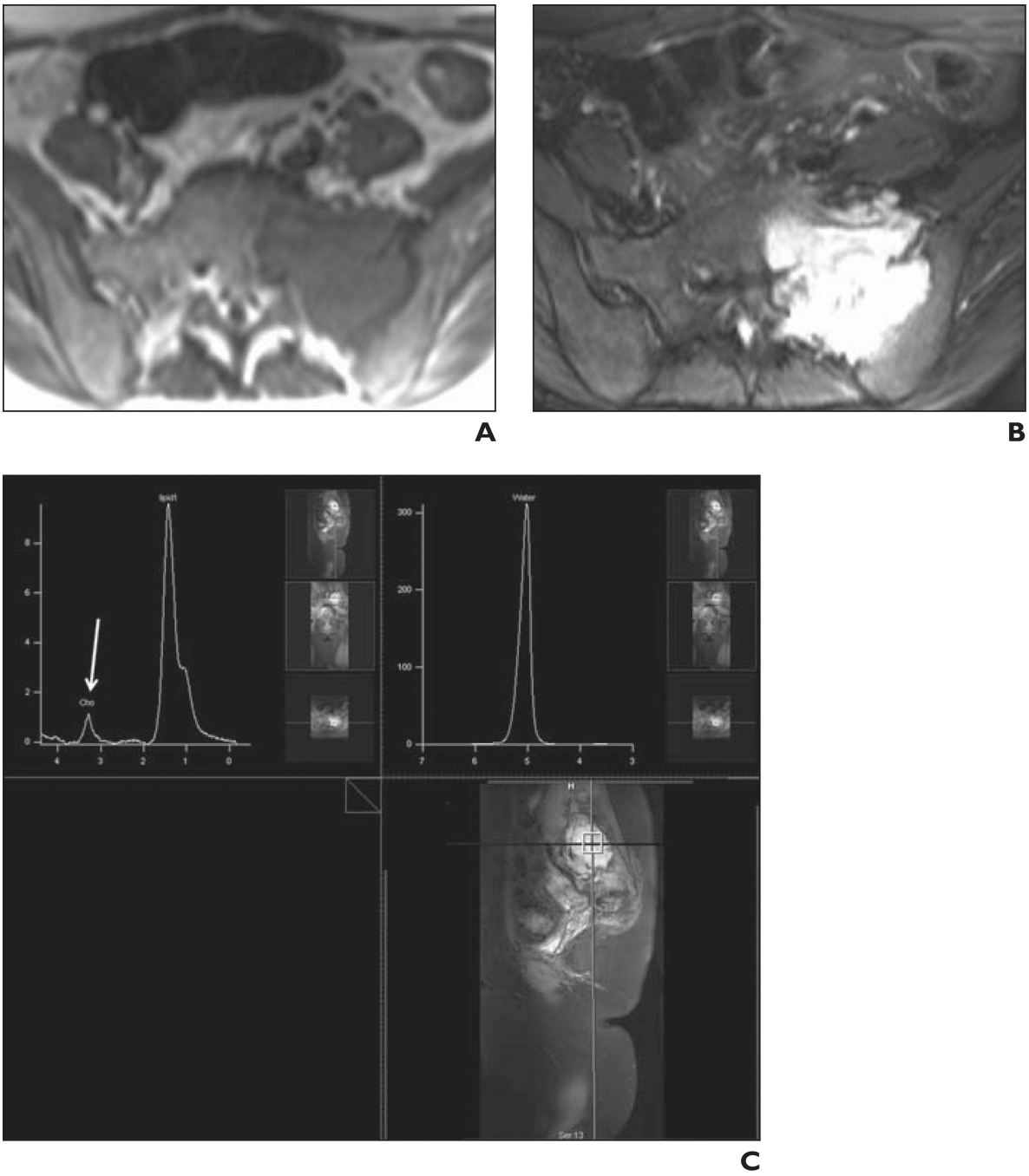

Figure 5.

25-year-old woman with Ewing sarcoma of left sacrum.

A, Axial T1-weighted spin-echo MR image (TR/TE, 690/15) shows left sacral mass as low-signal-intensity lesion at sacroiliac joint.

B, Axial fat-suppressed fast spin-echo T2-weighted MR image (TR/TE, 2886/100) shows involvement of neural foramina, crossing of sacroiliac joint, and associated soft-tissue component in anterior aspect. Although conventional MRI findings suggested malignant

features, diagnosis of giant cell tumor was entertained in light of some characteristic features.

C, Single-voxel proton MR spectroscopic map obtained within sacral mass with weak water suppression (*top left*) shows discrete choline peak (*arrow*). Relative signal-to-noise ratio is 3.6. Absolute choline concentration was calculated to be 2.9 mmol/kg, suggesting malignancy in this pathologically proven Ewing sarcoma. Upper right image is not water suppressed.

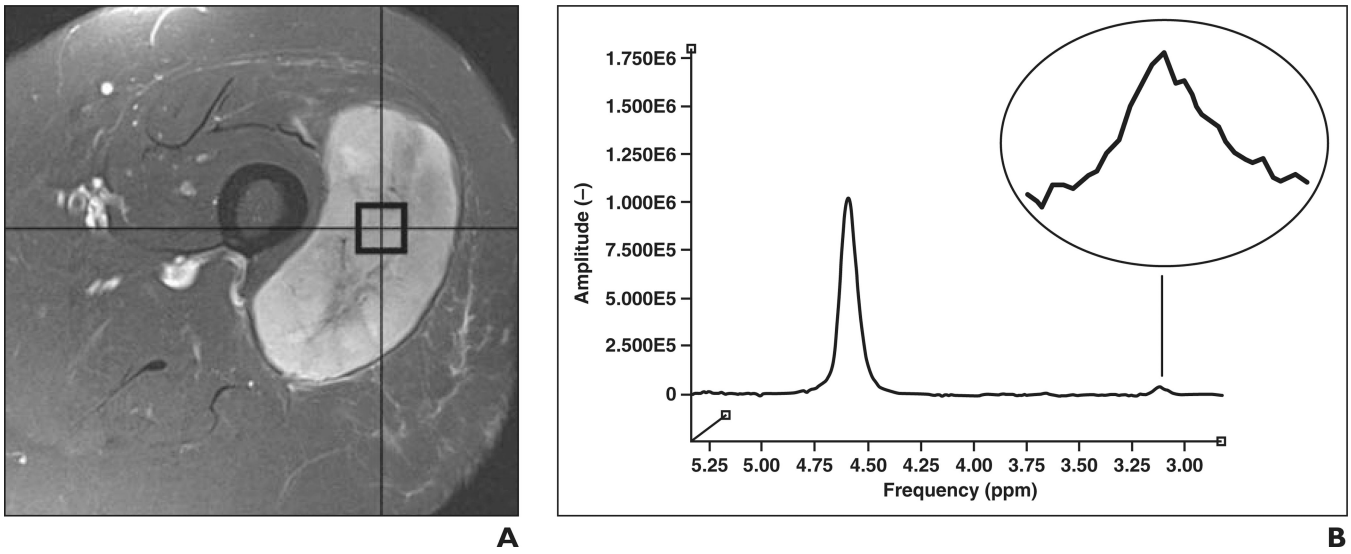

Figure 6.

81-year-old woman with high-grade soft-tissue sarcoma in lateral aspect of left thigh.

A, Axial fat-suppressed T2-weighted fast spin-echo MR image (TR/TE, 3030/64) shows circumscribed hyperintense mass centered on vastus lateralis muscle.

B, Single-voxel proton MR spectroscopic map obtained within mass with weak water suppression shows discrete choline peak (*inset*) with absolute choline concentration of 2.1 mmol/kg (reference, −4.6499E0).

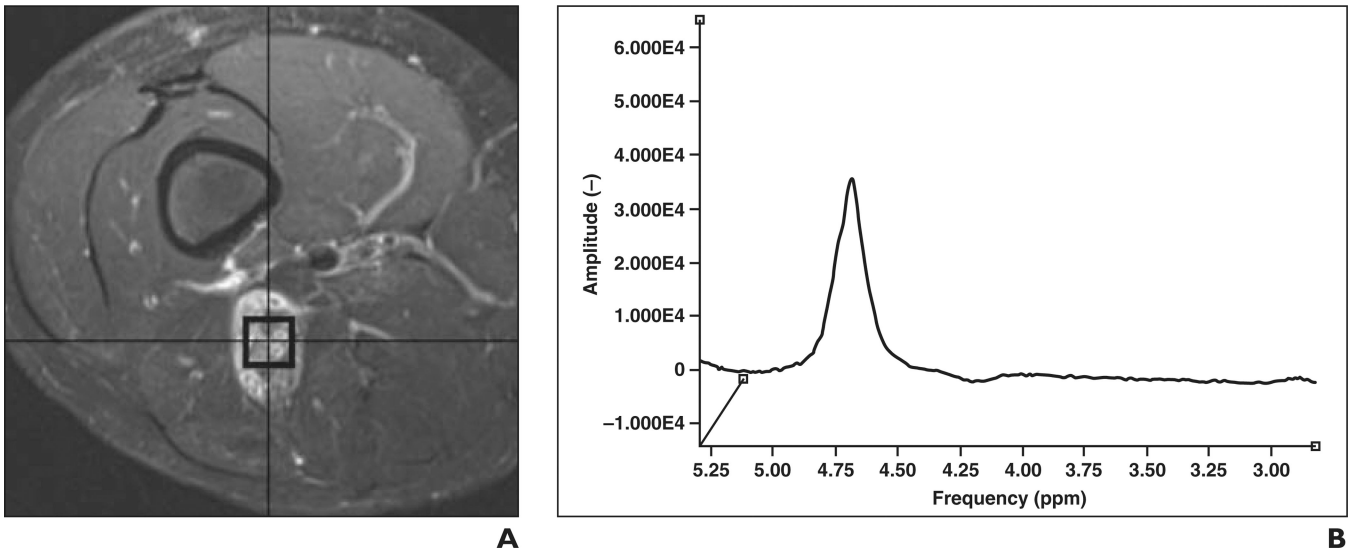

Figure 7.

11-year-old boy with neurofibromatosis type 1 and marked enlargement of right sciatic nerve caused by benign neurofibroma.

A, Axial fat-suppressed T2-weighted fast spin-echo MR image (TR/TE, 3600/71) shows mass.

B, Single-voxel proton MR spectroscopic map obtained within benign neurofibroma with weak water suppression shows no discernable choline peak at 3.2 ppm (reference, −4.7106E0).

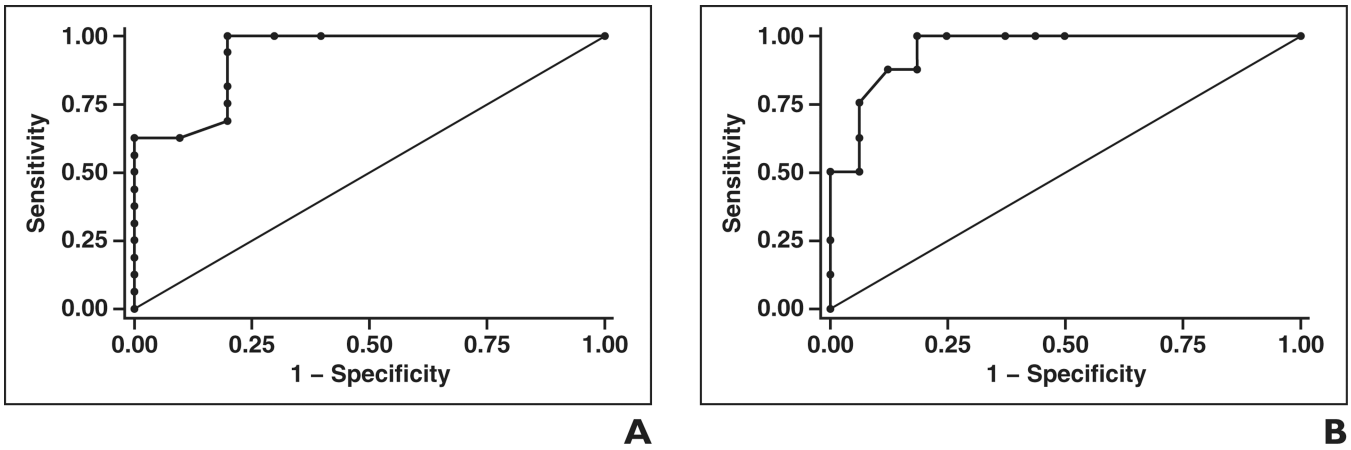

Figure 8.

Results of receiver operating characteristic analysis of characterization of musculoskeletal lesions as malignant on basis of semiquantitative and absolute quantitative metrics.

A and **B**, Graphs show receiver operating characteristic curves generated in 26 cases with choline signal-to-noise ratio (**A**) and in 24 cases with absolute choline concentration derived from proton MR spectroscopic data (**B**). Areas under each curve are large (**A**, 0.9281; **B**, 0.9492), allowing threshold choices of 5 for choline signal-to-noise ratio and 0.3 or 0.8 mmol/kg for absolute choline concentration, which are highly sensitive and relatively specific for malignancy (Table 4). Curves generated with Stata 11 software (StataCorp).

TABLE 1

Sample MR Spectroscopic Scan Protocol

Parameter	Water Suppression	No Water Suppression
Sequence	Point-resolved spectroscopy (single voxel)	Point-resolved spectroscopy (single voxel)
Lipid suppression	Not applied	Not applied
TR/TE	2000/135	2000/135
No. of signals acquired	128	16
Voxel size[a]	Variable	Variable
Acquisition time (min)	4	1

Note—Typical protocol for MR spectroscopic examination of masslike musculoskeletal lesion at our institution includes preliminary coronal STIR sequence with isotropic data resolution. The images are reconstructed into the axial and sagittal planes for localization. For calculation of choline concentration, both water-suppressed and nonsuppressed scans are necessary.

[a]Voxel size is prescribed according to size of the lesion. The smallest size used is $1 \times 1 \times 1$ cm^3, but the voxel is adjusted to encompass as much of the lesion as possible with careful exclusion of surrounding normal tissues.

TABLE 2

Summary of Technical Aspects of Reviewed Studies

Reference	No. of Lesions	Field Strength (T)	Voxel Count	TE	Acquisition	Choline Quantification Method	Analysis Method	No. f Technical Failures
Wang et al. 2004 [11]	36 in vivo untreated	1.5	Single	40,135,270	Water suppressed only	Qualitative: present or absent[a]	Nonquantitative	Not reported
Fayad et al. 2006 [4]	15 ex vivo specimens	1.5	Multiple	280	Water suppressed only	Signal-to-noise ratio	Simplex curve fitting	0
Sahetal. 2008 [12]	12 in vivo untreated	1.5	Single	30,135,270	Water-suppressed only	Qualitative: present or absent[b]	Nonquantitative	Not reported
Fayad et al. 2007 [5]	10 in vivo treated and untreated	3	Single and multiple	144	Water suppressed only	Signal-to-noise ratio	Simplex curve fitting	1[c]
Fayad et al. 2010[10]	15 in vivo untreated	3	Single	135	Water-suppressed and nonsuppressed	Concentration in mmol/kg (water as internal reference)	Internal water nonlinear least squares (advanced method for accurate, robust, and efficient spectral fitting algorithm in Java-based MR user interface software)	1[d]
Leeetal. 2010[8]	27 in vivo, status unclear	3	Single	144	Water-suppressed only	Concentration in mmol/kg[e]	LCModel (Inverse Problems)	Not reported
Fayad, unpublished data	7 in vivo untreated	3	Single	135	Water-suppressed and nonsuppressed	mmol/kg (water as internal reference)	Internal water nonlinear least squares (advanced method for accurate, robust, and efficient spectral fitting algorithm in Java-based MR user interface software)	0

Note—Studies included in meta-analysis of MR spectroscopic studies of musculoskeletal lesions. All studies were performed with point-resolved spectroscopy. Unless otherwise indicated, studies consisted of in vivo tumor evaluation with or without neoadjuvant therapy.

[a] Present indicates discrete choline peak on spectra from at least two TEs.

[b] Present indicates discrete choline peak on spectra from at least two TEs or choline signal-to-noise ratio > 2 in at least two TEs.

[c] Technical failure for unresected lesion; 2 of 10 additional postoperative examinations resulted in technical failure.

[d] Technical failure for unresected giant cell tumor of tendon sheath in wrist; 3 of 10 additional postoperative examinations resulted in technical failure.

[e] As published, but data allow extraction of only presence versus absence of a discrete choline peak for pooled analysis.

TABLE 3

Summary of Qualitative Analysis of 122 Musculoskeletal Tumors Analyzed With Proton MR Spectroscopy

Lesion	No. of Cases	
	Total	Discrete Choline Peak Present
Benign		
Abscess	1	1
Baker cyst	1	0
Bone cyst	3	0
Bursitis	1	0
Desmoid	2	0
Elastofbroma	1	0
Enchondroma	2	2
Fibrous dysplasia	2	1
Ganglion	2	0
Giant cell tumor	16	6
Giant cell tumor of tendon sheath	1	0
Granuloma	1	0
Hemangioma	3	0
Hematoma	3	0
Heterotopic ossifcation	1	0
Lipoma	5	0
Lipogranuloma	1	0
Nodular fasciitis	1	0
Pilomatricoma	1	0
Benign peripheral nerve sheath tumor	9	9
Stress reaction	1	0
Trichilemmal cyst	1	0
Tuberculous arthritis	1	0
Unknown[a]	2	1
Total	62	20
Malignant		
Chondrosarcoma	4	3
Epithelioid sarcoma	1	1
Ewing sarcoma	4	4
Fibrosarcoma	1	1
Fibromyxoid sarcoma	1	0
Hemangiopericytoma	1	0
Leiomyosarcoma	2	2
Liposarcoma	4	2
Lymphoma	2	2

Lesion	No. of Cases	
	Total	Discrete Choline Peak Present
Malignant fbrous histiocytoma[b]	3	3
Metastasis	18	18
Malignant peripheral nerve sheath tumor	3	3
Myofbroblastic sarcoma	1	1
Osteosarcoma	14	12
Synovial sarcoma	1	1
Total	60	53

Note—Seven cases have not been reported in the literature. Otherwise, only peer-reviewed studies that included a detailed list of tumor types and corresponding choline signal analysis were included [4, 5, 8, 10–12]. Imaging was performed at 1.5 and 3 T, with both single-voxel and multivoxel spectroscopic techniques, and varied in method of choline content analysis (qualitative analysis, relative quantification, or absolute quantification). The results of the studies in which quantitative results were reported were reclassified as categoric data (qualitative data reported as presence or absence of choline peak) to facilitate overall comparison.

[a]Two lesions reported as unknown but thought to be benign on basis of clinical and radiographic findings [5].

[b]For brevity the term malignant fibrous histiocytoma is used. This term has been changed to high-grade undifferentiated pleomorphic sarcoma in the World Health Organization classification.

TABLE 4

Summary of Performance of MR Spectroscopy of Musculoskeletal Lesions

Characteristic	Presence vs Absence of Discrete Choline Peak	Choline Threshold		
		Signal-to-Noise Ratio 5	Concentration 0.3 mmol/kg	Concentration 0.8 mmol/kg
No. of cases	122	25	24	24
Reference	4, 5, 8, 11, 12	4, 5	10 and unpublished data	10 and unpublished data
Sensitivity	0.88	0.81	1.00	0.88
Specificity	0.68	0.78	0.81	0.88
Positive predictive value	0.73	0.87	0.73	0.78
Negative predictive value	0.86	0.70	1.00	0.93

Note—Modest improvements in diagnostic performance of MRS for musculoskeletal lesions can be achieved with semiquantitative or absolute quantitative techniques, particularly with respect to specificity and negative predictive value. Although choline signal-to-noise ratio threshold performed well in this small sample size, as reported in the literature, the use of signal-to-noise ratio has well-known limitations and is sensitive to variations in the electrical conductivity of the receiver coil, microscopic field homogeneity in the voxel of interest, and the quality of shimming. Absolute choline concentration may be a more robust method of quantification.